



## Open Archive Toulouse Archive Ouverte (OATAO)

OATAO is an open access repository that collects the work of Toulouse researchers and makes it freely available over the web where possible.

This is an author-deposited version published in: <http://oatao.univ-toulouse.fr/>  
Eprints ID: 11260

**To cite this version:**

Raynal, Sylvain and Chatellier, Ludovic and David, Laurent and Courret, Dominique and Larinier, Michel *Numerical simulations of fish-friendly angled trashracks at model and real scale*. (2013) In: 35th IAHR World Congress, 08 September 2013 - 13 September 2013 (Chengdu, China).

Any correspondence concerning this service should be sent to the repository administrator:  
[staff-oatao@inp-toulouse.fr](mailto:staff-oatao@inp-toulouse.fr)

# Numerical simulations of fish-friendly angled trashracks at model and real scale

Sylvain Raynal

*PhD Student, Axe HydEE (Hydrodynamique et Ecoulements Environnementaux), Institut P', CNRS - Université de Poitiers - ENSMA, 86962 Futuroscope Chasseneuil, France.*

*Email: sylvain.raynal@univ-poitiers.fr*

Ludovic Chatellier

*Assistant Professor, Axe HydEE (Hydrodynamique et Ecoulements Environnementaux), Institut P', CNRS - Université de Poitiers - ENSMA, 86962 Futuroscope Chasseneuil, France.*

*Email: ludovic.chatellier@univ-poitiers.fr*

Laurent David

*Professor, Axe HydEE (Hydrodynamique et Ecoulements Environnementaux), Institut P', CNRS - Université de Poitiers - ENSMA, 86962 Futuroscope Chasseneuil, France.*

*Email: laurent.david@univ-poitiers.fr*

Dominique Courret

*Environmental Engineer, Pôle Écohydraulique ONEMA - IMFT - IRSTEA, Institut de Mécanique des Fluides de Toulouse, 31400 Toulouse, France. Email: dominique.courret@imft.fr*

Michel Larinier

*Senior Engineer. Email: michel.larinier@wanadoo.fr*

## **ABSTRACT:**

Several amphihaline species, such as silver eels, suffer high mortality rates during their downstream migration, due to their passage through turbines. The combination of adapted trashracks (inclined or angled screen, lower bar spacing, ...) with bypasses can efficiently prevent these mortalities. A numerical study has been carried out with such angled trashracks. Numerical results with model scale racks were validated against previous experimental results on model trashracks, resulting from head loss and velocity distribution measurements (Raynal et al., 2013). Real scale racks were then computed in order to evaluate the influence of both the bar spacing and the channel width on velocity distributions in real dimensions. The mesh generation and the numerical simulations were performed by the open source CFD software suite OpenFOAM. The trashrack solid comprised basic elements, individually created using CAD software and directly inserted in OpenFOAM's mesh generation utility. For small scale configurations, grid refinement was applied at the flume walls, at trashrack bars and downstream of the trashrack, whereas only bars were refined for real scale racks. The resulting number of cells ranged between 100,000 and 1,500,000. Steady state results were obtained by solving the Reynolds-averaged Navier-Stokes (RANS) equations for an incompressible and monophasic flow. The  $k-\varepsilon$ ,  $k-\varepsilon$ -based RNG,  $k-\omega$ ,  $k-\omega$ -based shear stress transport (SST) and Spalart-Allmaras models were examined to select the most appropriate one in terms of computation time and result accuracy. Results show that the  $k-\varepsilon$ -RNG is the model best agreeing with experimental results. Two-dimensional calculations seem to provide quite satisfactory results although both the head losses and the size of the recirculation zone downstream of the trashrack are slightly under-estimated. Real scale results confirm experimental ones and show that the bar spacing slightly effects upstream velocity profiles. Downstream of the rack, simulations with different flume width demonstrated that the size of the recirculation zone is proportional to the channel width.

**KEY WORDS:** Fish-friendly trashracks, Head loss, Numerical Modeling, RANS, Velocity distributions.

## 1 INTRODUCTION

Fish mortality caused by turbines at hydropower plants during their downstream migration has become a worldwide concern in the last decade. In Europe, the European Water Framework Directive (2000/60/EC), the European Council regulation (no. 1100/2007) for the recovery of eel (*Anguilla Anguilla*) and restoration plans for amphibiotic species such as salmon (*Salmo salar*) or sea trout (*Salmo trutta*), have focused on the need to avoid or at least minimize these mortalities. Among the few answers, fish-friendly screens remain one of the main feasible. Indeed, conventional trash racks can be adapted into fish-friendly ones by reducing the bar spacing and either by inclining the rack from the ground, or by angling the rack from the wall. In both cases, the aim is to guide fish towards bypasses, located at the downstream end of the rack, by generating tangential currents.

Studying these racks requires studying both the biological aspects (guidance along the rack, possible impingement) and the economical ones (energy loss through the rack, homogeneity at the turbine entrance). Several numerical and/or experimental studies focused on some of these aspects in the case of angled trashracks.

Ghamry and Katopodis (2009) numerically modeled free-surface water flowing through a rack. They compared their results with experimental ones, obtained by PIV (Particle Image Velocimetry) by Tsikata et al. (2007). These experiments mainly focused on velocities in the vicinity of the rack. Their racks comprised from 3 to 5 bars and had a slight angulation with  $\alpha$  ranging from  $90^\circ$  (perpendicular rack) to  $78^\circ$ . Ghamry and Katopodis used the ANSYS CFX-11.0 CFD application to model a 3-D free surface turbulent flow using a 1 million cell mesh. They compared the performance of seven turbulence models (standard  $k-\varepsilon$ , standard  $k-\omega$  ...). Five criteria including water levels, velocities and computational time, were selected to compare numerical and experimental results. On the whole, head losses were rather well predicted as well as velocities in the vicinity of the rack. Downstream of bars, velocity predictions differ somewhat from PIV measurements. The comparison with experiments revealed that the  $k-\omega$ ,  $k-\varepsilon$  and eddy viscosity transport models produce the best prediction. Finally, the  $k-\omega$  was selected for other investigations since it showed slightly faster computational time.

Other studies are centered on the flow behavior around trashracks, without focusing on modeling the flow in the vicinity of the rack. Indeed, trashracks or fish screens may be modeled as porous media in order to lower the number of cells. Khan et al. (2004) numerically modeled the entrance of a hydropower plant (Star-CD software, high  $Re$   $k-\varepsilon$  turbulence-closure model) and simplified the rack with this technique. Ho et al. (2011) also used a similar numerical modeling and replaced angled wedge-wire screens and perforated plates by porous media with directional porosity (Flow3D software,  $k-\varepsilon$  turbulence-closure model). Even with these simplifications, both studies resulted in numerical results in good agreement with experimental observations.

Chatellier et al. (2011) and Raynal et al. (2013) experimentally investigated model angled racks with bars scaled down to half size. Different racks angles  $\alpha$  ( $\alpha = 30^\circ, 45^\circ, 60^\circ$  or  $90^\circ$ ) and different bar spacings  $e$  ( $e/b = 1, 1.5, 2$  or  $3$  where  $b$  is the bar thickness) were tested in order to assess the effect of these parameters on both head losses and velocity distributions. They especially implemented ADV (Acoustic Doppler Velocimetry) and PIV systems in order to measure velocities around these racks. Results revealed that the upstream flow accelerated towards the end of the trashrack. At  $\alpha = 45^\circ$ , the axial velocity  $U$  increased up to 70% above the upstream mean velocity  $V_I$ . Downstream of the rack, the flow was asymmetric with a fairly large recirculation zone. The bar spacing and the bar shape had only a slight effect on upstream velocity profiles. For rectangular shaped bars, differences were up to 20% in the downstream part of the rack.

The present study focuses on calculations with angled racks, at both model and real scale. Experimental results from Chatellier et al. (2011) and Raynal et al. (2013) studies are used to validate computational results. Simulations with different turbulence models at model scale are performed to select the parameters producing the best agreement with experiments. Real scale simulations are then done in order to analyse the effect of the channel size or of the bar spacing on the velocity distribution upstream and downstream of the rack.

The second section of this paper explains the numerical parameters and describes the experimental results used for verification. The third section compares the efficiency of various turbulence-closure models in terms of head loss and velocity distribution predictions. Then, the best turbulence model is used

in real scale simulation to analyze the influence of the bar spacing and the channel width's one on velocity profiles. All these results are then discussed and recommendations are made for the design of fish-friendly water intakes with angled trashracks.

## 2 NUMERICAL MODELING

This study focuses on two trashrack scales. First, computational results with model scale racks are compared with previous experimental results in order to validate the use of 2D turbulent flow with OpenFOAM in the context of this study, i.e. fish-friendly angled trashracks. Then, real scale racks are simulated to complete experimental results.

### 2.1 Experimental configurations selected for verification

Experimental results are extracted from Chatellier et al. (2011) and Raynal et al. (2013) studies. They performed an experimental investigation on model angled trashracks, with various rack angles (from  $\alpha = 90$  to  $30^\circ$ ), bar spacings (from  $e/b = 1$  to 3) and 2 bar shapes. Bars were half-scaled and were 5 mm wide by 40 mm deep. In addition, trashracks also comprised spacer lines and two lateral pieces, triangular shaped, used to hold the rack to the channel. The rack was inserted in a 0.6 m ( $B$ ) wide open water channel, in which water flowed at  $Q = 130$  l/s. Water depths were generally set at 350 mm leading to upstream mean velocities  $V_l$  around 0.7 m/s. During this study, head losses were measured and velocity profiles were acquired at mid-depth with an Acoustic Doppler Velocimeter probe. These values are added to those measured on similar configurations with a PIV system by Chatellier et al. (2011).

For the present study, two configurations, meeting fish-friendly criteria, have been selected for computations. Simulated racks are angled at  $\alpha = 45^\circ$ , comprise bars spaced by 10 mm (corresponding to 20 mm in real size), and have either a rectangular ( $PR$ ) or a more hydrodynamic cross-section ( $PH$  - illustrated in Figure 1). Head loss values and velocity profiles, measured in these two configurations, are detailed in section 3.2.

### 2.2 Mesh and numerical geometries

#### 2.2.1 Model scale racks

Since model scale simulations are compared with experimental ones, model scale rack geometries need to be very close to those used during experiments. Simulated model racks comprised two specific lateral pieces and 51 bars, 5 mm thick ( $b$ ) and 40 mm deep ( $p$ ), spaced by  $e = 10$  mm (Figure 1). Since simulations were two-dimensional, spacer lines could not be modeled. The rack, whose upstream end is placed at the origin of the coordinate system, is inserted in a 0.6 m wide domain which starts at  $x = -3$  m and ends at  $x = 4$  m (the rack ends at  $x = 0.6$  m).

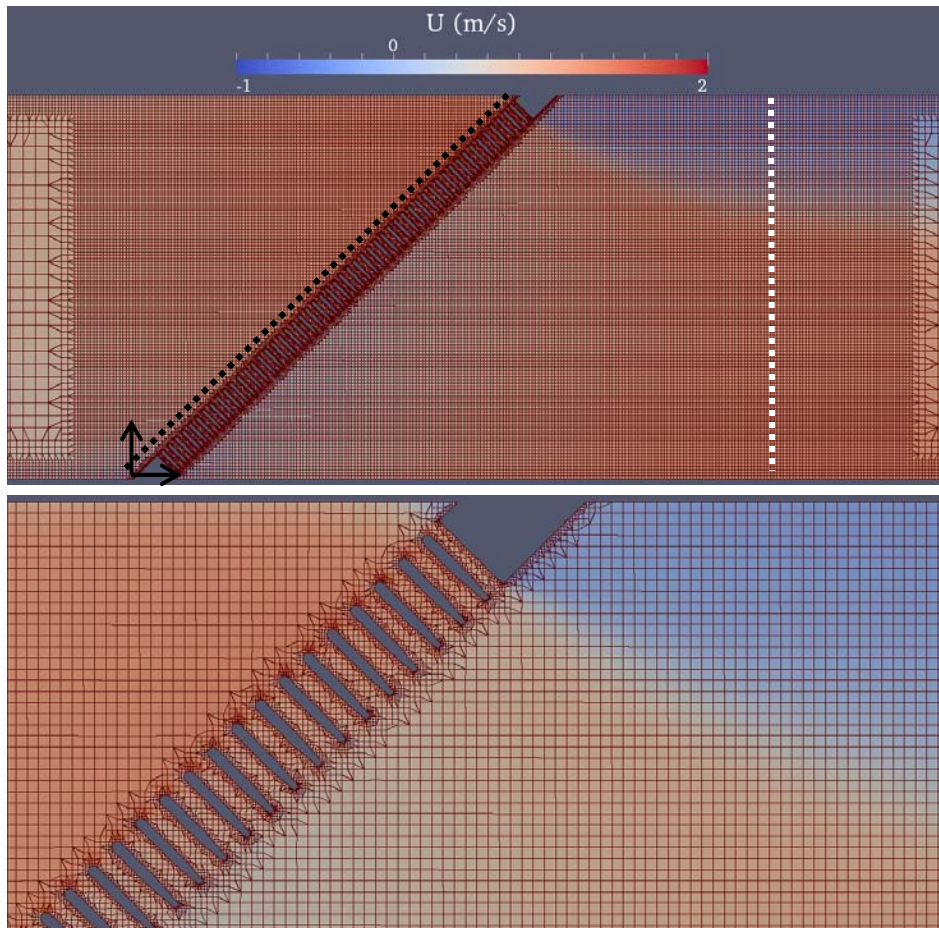


**Figure 1** Full-width (top) and zoomed (bottom) view of computed mesh for small scale racks, superimposed with resulting velocity fields (inlet velocity is uniformly set at 0.7 m/s). Bars are profiled (*PH*) with a rounded leading edge and a thin trailing edge. Velocity profiles, extracted for comparison at 20 mm from the rack (black dashed line) and downstream of the rack at  $x = 1$  m (white dashed line), are also illustrated. Black arrows represent the coordinate origin.

### 2.2.2 Real size racks and water intakes

Real size racks also comprise bars and lateral pieces. Only rectangular bars are simulated. Bars are real scaled and are consequently 10 mm wide and 80 mm deep. The rack was also inserted at the origin of the coordinate system. Moreover, in all the real size configurations, the domain started at  $x = -B$  and ended at  $x = 3B$ .

The first kind of simulations focused on the effect of the bar spacing  $e$  on velocity profiles. The channel width was set at  $B = 10$  m and the bar spacing was alternatively set at  $e = 10, 20$  and 30 mm, leading to  $e/b$  ratios from 1 to 3.

The second type of computations was centered on the effect of the channel width on velocities. The bar spacing was fixed at  $e = 20$  mm, and the channel width was alternatively set at  $B = 5, 10$  and 30 m.

## 2.3 Mesh generation

### 2.3.1 Channel

The mesh was generated with the same OpenFOAM functionalities for both model and real scale simulations. The channel geometry is initially modeled as a coarse, structured, uniform rectangular mesh comprised of hexahedral cells. The chosen cell size represents the coarsest level of the mesh, also

denominated as level “0”. Incrementing the mesh level amounts to halving all the cell dimensions.

### 2.3.2 Trashrack

The trashrack geometry was generated in two phases.

First, basic elements were created with CAD software. Then, according to selected parameters (channel width, bar spacing, bar width,...), the trashrack elements are scaled, rotated, and assembled using a C++ code.

Afterwards, this rack was inserted and meshed by the OpenFOAM’s mesh castellation utility snappyHexMesh. Two complementary functions were used for mesh refinement: the mesh level around the inserted geometry, i.e. the trashrack, was specifically fixed and sub-domains, in which the mesh level was incremented, were created. All the mesh levels and increments refer to the level “0” defined during the channel geometry definition, and result in refined hexahedral and semi-hexahedral cells.

### 2.3.3 Mesh levels

Mesh levels were always the same for *PR* and *PH* racks. Table 1 compares some geometry and mesh parameters and also gathers refinement levels for both scales.

For real scale racks, the large number of bars prevented from having a very refined mesh and only bars were refined. Near bars, the size of the cell was around 1.5 mm.

For model scale racks, which comprise fewer bars, other zones were refined. Bars were refined with a cell size around 0.6 mm. In addition, longitudinal bands were refined near the channel sides in order to have good near-wall treatment. Typically, the band width was around  $B/20$  (30 mm). Moreover, mesh refinement was also applied in the trashrack wake, over the whole channel width and until  $x = 2B$ .

**Table 1** Mesh and geometry descriptions for small and real scale configurations

		Model scale geometry	Real scale geometry
Channel width $B$ (m)		0.6	10 *
Bar thickness $b$ (m)		0.005	0.010
Number of bars		51	467 *
Number of cells		100,000	500,000 *
Size of level 0 cells (m)		0.020	0.100
Refinement levels	Channel sides	2	0
	Bars	5	6
	Trashrack wake	2	0
* For real scale configurations, these values depend on the channel width $B$			

### 2.4 Governing equations

Simulations were performed with OpenFOAM software, and using the “simpleFoam” solver, dedicated to stationary, turbulent and monophasic flows. The three dimensional (restricted to two dimensions using a single mesh layer the  $z$ -direction) Reynolds-averaged Navier-Stokes (RANS) equations were solved and were alternatively coupled with five turbulence-closure models:

- the  $k-\varepsilon$  developed by Launder and Spalding (1974)
- the  $k-\varepsilon$  based RNG method (renormalization group) by Yakhot et al. (1992)
- the  $k-\omega$  by Wilcox (1988)
- the  $k-\omega$  based SST (shear stress transport) by Menter (1994)
- the Spalart and Allmaras (1992) model

Apart from the last one, all these turbulence models are two equation ones. Governing equations or detailed descriptions of these models can be found in original papers or in other studies such as Pope (2000) or ASCE task committee (1988).

## 2.5 Boundary conditions and initials values

Boundary conditions were the same for both model and real scale simulations. A symmetry condition is applied on top and bottom faces, leading to vertical velocities  $W = 0$  m/s in the whole domain. At the inlet, a uniform velocity value is set at  $U = 0.7$  m/s (corresponding to  $V_I$  during experiments). Since only relative pressures are calculated by this solver, the pressure inlet value was set at 0. Bars and flume sides are considered as walls, with no-slip conditions. Specific near-wall functions, already implemented in OpenFOAM, were applied around these faces. At the outlet, zero gradient boundary conditions were applied on all variables.

Moreover, for each variable of the different turbulence models ( $k$ ,  $\varepsilon$ ,  $\omega \dots$ ), different initial values were tested. However, they had no significant effect on the final results and are not detailed herein.

## 3. SMALL SCALE COMPARISONS

### 3.1 Procedure

Model scale simulations aimed at selecting the best turbulence model for this study. Two main criteria were selected: computational time and agreement between experimental and numerical results. This second point is centered on three salient results:

- The head loss generated by the rack. In single phase numerical tests, head losses account for pressure differences only. Pressure values are extracted at  $x$ -positions similar to those where water levels were experimentally measured (upstream and downstream pressures are extracted at  $x = -1$  m and  $x = 2.5$  m respectively).
- The velocity distribution along the rack. Velocities are extracted at 20 mm from the rack in both numerical tests (black line in Figure 1) and PIV images.
- A transverse profile downstream of the rack highlighting the recirculation zone. As PIV images do not provide data further than  $x = 1$  m, transverse velocity profiles are extracted at  $x = 1$  m in numerical tests (white line in Figure 1).

### 3.2 Results

Upstream and downstream velocity profiles are compared in Figure 2 in order to assess the performance of each turbulence-closure model.

For velocity profiles along *PR*-racks, all turbulence models produce good predictions, reproducing the flow acceleration towards the end of the trashrack. Only slight differences occur between these models. Along *PH*-racks, velocities are over estimated with all turbulence models in the downstream half of the rack. One can hardly determine which model results in the best predictions of upstream velocity profiles. Indeed, only slight differences occur between upstream velocity profiles and there is no model resulting in good predictions for both bar shapes

Downstream of each rack, the three dimensional behavior of the flow observed experimentally increases the differences between numerical predictions and measured velocities. Experiments show a recirculation zone extending on the left bank ( $y = 600$  mm) until around  $y = 300$  mm. The size of this recirculation is under estimated by all the turbulence models and for both bar shapes. Moreover, the  $k-\omega$ ,  $k-\omega$ -SST and Spalart-Allmaras models seem to predict a velocity peak near the recirculation zone (around  $y = 0.37$  m) which was not observed in measured velocity profiles. Nonetheless, downstream of *PH*-bars, the  $k-\varepsilon$ -RNG model produces the best estimation of the width of the recirculation zone.

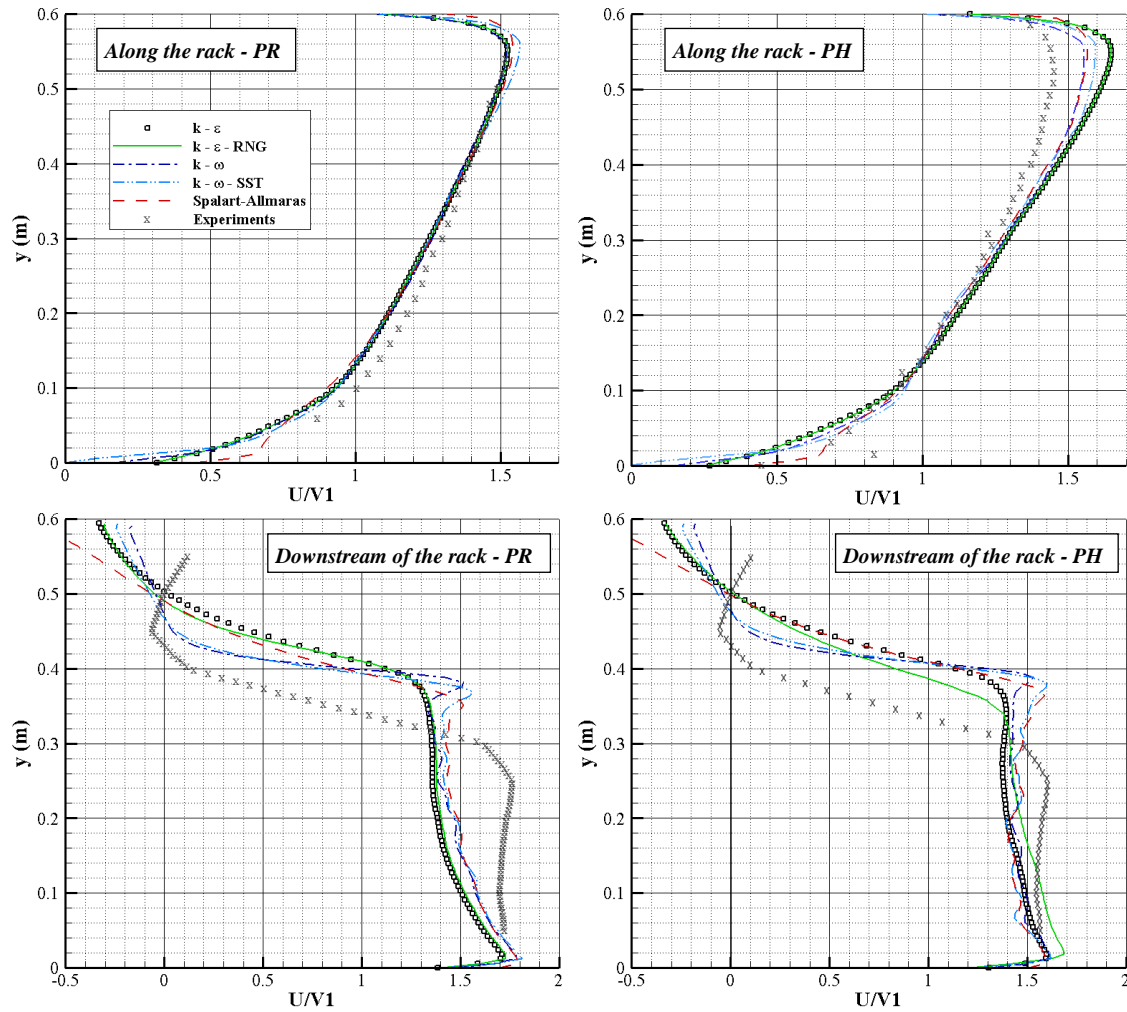


**Figure 2** Velocity profiles along (top) and downstream of the rack (bottom) angled at  $\alpha = 45^\circ$ . Bar section is either rectangular (*PR* – left) or more hydrodynamic (*PH* – right). Velocities are normalized by the upstream mean velocity  $V_I$ .

Head loss values and computational times, which are the other comparative criteria, are gathered in Table 2. In both configurations, head losses are under-estimated by numerical results. This can be explained by 3D patterns which cannot be modeled in such 2D simulations. Moreover, spacer lines, which block a fraction of the water depth, were not taken into account in these computations.

Nevertheless, despite these numerical simplifications, some models result in good head loss predictions with errors lesser than 10%. The  $k-\omega$  and  $k-\varepsilon$ -RNG models are those best predicting head losses for *PR* and *PH* bars respectively. On the contrary, the Spalart-Allmaras model produces the most under-estimated values.

However, if the  $k-\omega$  and the  $k-\varepsilon$ -RNG prediction accuracies are rather similar, computational times are very different. Indeed, the  $k-\omega$  model computational time, which was around five times as long as the  $k-\varepsilon$ -RNG one, finally appeared to be prohibitive.



**Table 2** Comparison of head loss coefficient predictions and computational time for small scale configurations. For each head loss numerical prediction, deviation from the experiments is written in brackets. The experimental uncertainty is also detailed for both bar shapes.

Turbulence models	Head loss coefficient $\zeta$		Computational time
	PR	PH	
$k-\varepsilon$	2.8 (-15%)	2.19 (-9%)	<b>x 1.0</b>
$k-\varepsilon$ -RNG	2.83 (-14%)	<b>2.24 (-7%)</b>	<b>x 1.0</b>
$k-\omega$	<b>3.02 (-8%)</b>	2.2 (-8%)	x 5.0
$k-\omega$ -SST	2.93 (-11%)	2 (-17%)	x 5.0
Spalart-Allmaras	2.76 (-16%)	1.97 (-20%)	x 1.3
<b>Experiments</b>	<b>3.3 <math>\pm</math> 6%</b>	<b>2.4 <math>\pm</math> 8%</b>	--

In conclusion, all these five turbulence models result in relevant simulations. Nonetheless, results show that the  $k-\varepsilon$ -RNG model should be the best one for this study. Indeed, it is the fastest one and, on the whole, it best predicts velocity fields and head loss coefficients.

#### 4. REAL SCALE SIMULATIONS

##### 4.1 Extracted profiles

There are two main objectives in this fourth section focusing on real scale racks (Figure 3). First, simulations should help to determine the influence of the channel width  $B$  on velocity profiles, because  $B$  could not be changed during experiments. Secondly, simulations should also make it possible to determine the effect of the bar spacing on velocity profiles in real dimensions.

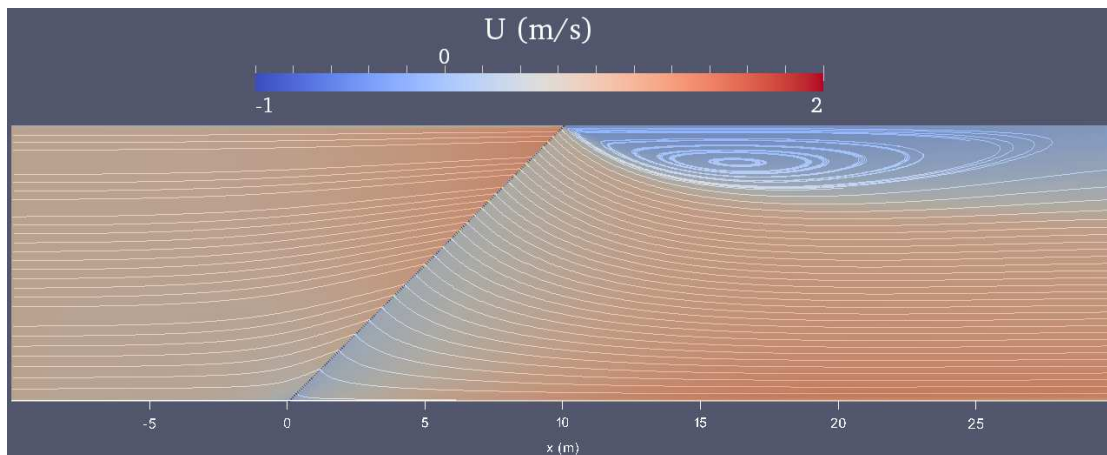


**Figure 3** Whole domain for real scale computations with  $B = 10$  m. Velocity fields are superimposed with streamlines (inlet velocity is 0.7 m/s). The  $x$ -axis is represented at the bottom of the domain. Downstream velocity profiles are extracted at  $x = 15, 20$  and  $25$  m.

This analysis is entirely achieved by centering on four velocity profiles extracted from computed results. Upstream velocities have been extracted along the rack, at 200 mm from bars. Downstream of the rack, three transverse velocity profiles have been extracted at  $x = 1.5B, 2B$  and  $2.5B$ . Since the recirculation size may depend on the channel width, the axial position of downstream profiles was decided to be proportional to  $B$ . On the contrary, upstream of the rack, velocity profiles are more affected by the bar dimensions (which is the same in all configurations). Moreover, this order of magnitude (few decimeters) corresponds to recommended distances to describe velocity fields in front of screens with respect to fish guidance and impingement risks (USDI 2009, EA 2012).

## 4.2 Results

Figure 4 compares upstream and downstream velocity profiles for real scale trashracks with different bar spacings and different channel widths. These  $U/V_I$  profiles are drawn against the coordinate  $y$ , normalized by the channel width  $B$ .

As observed experimentally, upstream velocity profiles are somewhat influenced by the bar spacing. When bars are closer, velocities tends to be lower in the downstream part of the rack. Velocity differences may range up to 10-15%. These differences tend to vanish downstream of the rack.

On the other hand, there is nearly no effect of the channel width on velocity profiles (drawn against  $y/B$ ). This especially means that the width of the recirculation zone downstream of the trashrack is proportional to the channel width. For example, at  $x = 2B$ , axial velocities significantly decrease for all configurations for  $y/B > 0.65-0.70$  and become negative for  $y/B > 0.85-0.90$ . Similar commentaries can be made for the length (along the  $x$ -direction) of this recirculation zone. Indeed, the good agreement between velocity profiles at  $x = 2B$  was also true for  $x = 1.5B$  and  $x = 2.5B$  (not shown in Figure 4), meaning that the size of the recirculation zone is proportional to the flume width  $B$  in both the  $x$  and  $y$  directions.

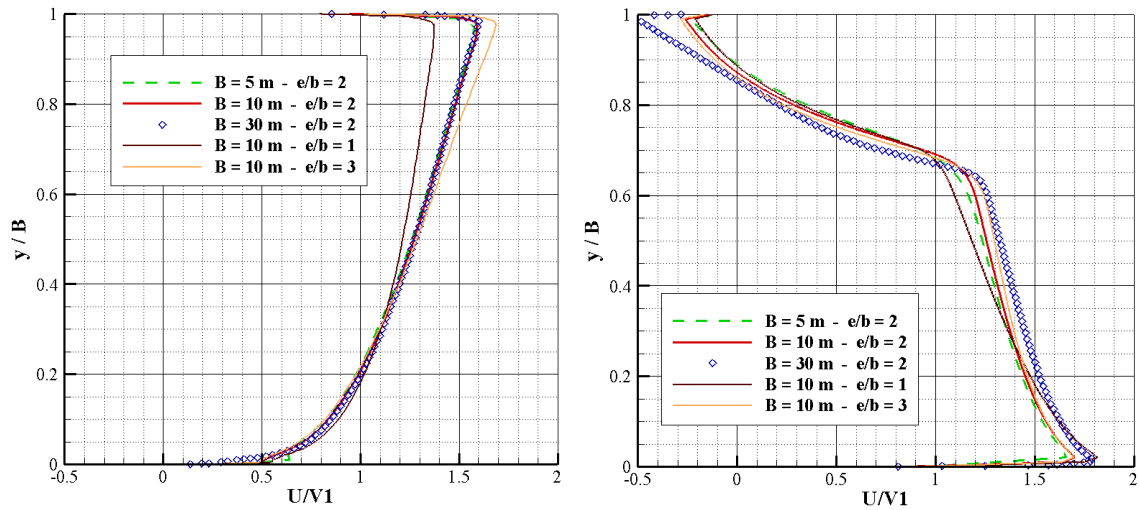


**Figure 4** Velocity profiles along (left) and downstream of the rack at  $x = 2B$  (right). On the vertical axis, the transverse coordinate  $y$  is normalized by the channel width  $B$ . Horizontally, axial velocities are normalized by the upstream mean velocity  $V_I$ .

## 5. CONCLUSION

This study focused on two-dimensional numerical simulations of angled trashracks at both model and real scale. Two configurations angled at  $45^\circ$ , which were experimentally investigated by Chatellier et al. (2011) and Raynal et al. (2013), were selected for this study.

Numerical results at the same model scale were compared to these experimental results. Head losses predicted with simulations are slightly under-estimated. The two main reasons may be the absence of spacer lines or the two-dimensional simplification for these simulations. Nonetheless, the best turbulence closure models produce head loss estimations with more than 90% accuracy. Concerning computed velocities, upstream profiles are in good agreement with the experimental ones but, downstream of the rack, velocity fields are less satisfactory. Even if all the turbulence models generate a recirculation zone, computed velocity profiles are quite different from experimental ones. Indeed, the size of the recirculation zone is under-estimated and some turbulence models generate odd velocity features (velocity peaks, ...).

On the whole, the five turbulence models finally resulted in rather similar results. Nevertheless, the  $k-\omega$  and  $k-\varepsilon$ -RNG models were the best predicting ones. However, since simulation durations with the  $k-\varepsilon$ -RNG model were five times as fast as those with the  $k-\omega$  one, the  $k-\varepsilon$ -RNG model was selected for large scale simulations. This remains coherent with other studies which also chose  $k-\varepsilon$  based models (Ho et al. 2011, Khan et al. 2004). However, some studies like Gharmy and Katopodis (2009), who investigated trashrack configurations with rather low blockage ratio, identified the  $k-\omega$  model as the best predicting one.

Still, in most studies focusing on trashracks, accurate numerical predictions require two equation turbulence closure models.

In summary, these model scale simulations validate the use of two dimensional computations to simulate fish-friendly angled trashracks. Although computed results somewhat differ from experimental ones, the main features are simulated and computational results remain relevant.

Real scale computations confirm some experimental results observed in small scale configurations. Bar spacing may influence the upstream velocity distribution along the rack. More especially, velocities are mainly different in the downstream end of the rack. Differences between  $e/b = 1$  and  $e/b = 3$  may range up to 20%. However, these differences tend to decrease downstream of the rack. Concerning the effect of the channel width, these computations also demonstrated that both upstream and downstream velocity profiles, drawn against  $y/B$ , are not affected by the channel width  $B$ . In particular, it was showed that the size of the recirculation zone is proportional to  $B$ .

All these conclusions, arising from this numerical study, complete previous experimental results on angled trashracks. They especially provide information at real scale and help to better understand the flow behavior downstream of the rack where highly asymmetric flows are generated. This recirculation zone, which can be penalizing for hydraulic operators, must be taken into account during water intake design phases.

## ACKNOWLEDGEMENT

This work was funded by the European Regional Development Fund (ERDF), the Région Poitou-Charentes, ONEMA, ADEME, CNR, SHEM and EDF. Their support is greatly appreciated.

## References

- ASCE Task Committee, 1988. Turbulence modeling of surface water flow and transport: Part I, II, III, IV and V. *Journal of Hydraulic Engineering*, 114(9), 970-1073.
- Chatellier L., Wang R.W., David L., Courret D. and Larinier M., 2011. Experimental characterization of the flow across fish-friendly angled trashrack models. *Proceedings 34th IAHR Congress Brisbane*, 2776-2783.
- Environment Agency, 2012. *Hydropower Good Practice Guidelines. Screening requirements.* (<http://www.environment-agency.gov.uk/business/topics/water/126575.aspx>).
- Ghamry H. and Katopodis C., 2009. A numerical investigation to select a turbulence-closure model for simulating turbulent flows near trashracks (bar racks). *Proceedings 33th IAHR Congress Vancouver*, 4045-4054.
- Khan L.A., Wicklein E.A., Rashid M., Ebner L.L. and Richards N.A., 2004. Computational fluid dynamics modeling of turbine intake hydraulics at a hydropower plant. *Journal of Hydraulic Research*, 42(1), 61-69.
- Launder B.E. and Spalding D.B., 1974. The numerical computation of turbulent flows. *Computational Methods and Applied Mechanics Engineering*, 3, 269-289.
- Menter F.R., 1994. Two-equation eddy-viscosity turbulence models for engineering applications. *AIAA Journal*, 32 (8), 1598-1605.
- Pope S.B., 2000. *Turbulent flows.* Cambridge University Press, UK.
- Raynal S., Chatellier L., Courret D., Larinier M. and David L., 2013. An experimental study in fish-friendly trashracks – Part 2. Angled trashracks. *Journal of Hydraulic Research*, 51(1), 67-75.
- Spalart P.R. and Allmaras S.R., 1992. A one-equation turbulence model for aerodynamic flows. *AIAA Paper*, 92-0439.
- US Department of Interior, 2009. *Guidelines for Performing Hydraulic Field Evaluations at Fish Screening Facilities.* ([http://www.usbr.gov/pmts/hydraulics\\_lab/pubs/manuals/Guidelines for Fish Screening Evaluations.pdf](http://www.usbr.gov/pmts/hydraulics_lab/pubs/manuals/Guidelines%20for%20Fish%20Screening%20Evaluations.pdf)).
- Wilcox D.C., 1988. Multiscale model for turbulent flows. *AIAA Journal*, 26, 1311-1320.
- Yakhot V., Orszag S.A., Thangam S., Gatski T.B. and Speziale C.G., 1992. Development of turbulence models for shear flows by a double expansion technique. *Physics of Fluids A: Fluid Dynamics*, 4(7), 1510-1520.